JOURNAL OF GEOPHYSICAL RESEARCH, VOL. 98, NO. B11, PAGES 19,687–19,703, NOVEMBER 10, 1993

MODELING OF VOLCANIC TREMOR AS EXPLOSIVE POINT SOURCES IN A SINGLE-LAYERED, ELASTIC HALF-SPACE

Evgenii Gordeev

Institute of Volcanology, Petropavlovsk-Kamchatsky, Russia

Abstract. I investigate path effects on the waveform of a volcanic tremor using a model that consist of an impulsive dilatational point source embedded in a single-layered, elastic half-space. Such a source may arise during a variety of volcanic conditions, such as a sequence of rapid explosions at a volcanic vent as well as gas-piston activity observed in basaltic lava lakes. Using acoustic signals recorded during the 1975 Tolbachik eruption, the 1983 Klyuchevskoy eruption, and the 1989 Tokachi-dake eruption, I propose a general impulsive time function for the tremor source, consisting either of a single impulse or a sequence of identical impulses. Computed seismograms illustrate the influence of a low velocity, surface layer on the shape and spectra of the waveforms. For the same layered model, a single impulse produces a dispersive wave, while a sequence of identical impulses produces a wave of multiple harmonics. For a single impulse, the peak in the seismograms shifts to higher frequencies when the surface layer is very thin. For multiple impulses, spectral peaks shift to higher frequencies as the time between successive impulses increases, indicating an increasing importance of higher-order harmonics.

Introduction

A nearly harmonic oscillation of the ground, commonly called volcanic tremor, has been recorded and intensely studied at many active volcanoes. Most people assume the energy source of tremor is caused by sudden expansion of a gas phase in magma. The assumption is easily supported when it is possible to record simultaneously an acoustic wave in the atmosphere produced by a surface explosion and a coincident seismic event [McNutt, 1986; Gordeev et al., 1990; Okada et al., 1990]. In this case, the seismic event is emergent, the so-called b-type events according to the Minakami classification of volcanic earthquakes [Minakami, 1960]. When a tremor is unrelated to specific surface events, the energy source is still often considered to be related to sudden gas expansion, which may excite a resonance in the magma system [Seidl et al., 1981; Cosentino et al., 1982; Schick, 1988].

Paper number 93JB00348.
0148-0227/93/93JB-00348$05.00

The harmonic character of some volcanic tremors may arise as a result of resonance of magma-filled cavities [Kubotera, 1974; Aki et al., 1977; Aki and Koyanagi, 1981; Chouet, 1981,1985; Crosson and Bame, 1985; Chouet, 1988] or instability in two-phase flow, as when magma degases [St.Lawrence and Qamar, 1979; Seidl et al., 1981; Ferrick et al., 1982]. How might it be possible to produce a harmonic seismic wave by a single explosion or, even, by a sequence of explosions? What is the influence of the pathway between the source and the surface on the possible character of volcanic tremor?

I consider the possibility that the harmonic character may be a related to the pathway between a source and the surface, in particular, dispersal of seismic waves through a thin low-velocity layer composed of friable and broken material that blankets many volcanic areas. I compute surface waveforms using a technique developed by Fatyanov [1980] and Fatyanov and Mikhailenko[1988], which enables me to solve the elastic equations that describe the propagation of seismic waves through a layered material for a dilatational point source.

Calculation of Waveforms and Choice of the Source Time Function

The waveform of a point source embedded in a layered half-space can be determined by solving the familiar elastic equations of motion [e.g., Jaeger, 1969]. In my specific model, each layer has constant elastic parameters. Assuming a traction-free surface and continuous displacement between layers, the equations can be solved by the method of finite integral transformations applied to the spatial and temporal variables [Fatyanov, 1980; Fatyanov and Mikhailenko, 1988]. The vector surface displacement $U(r,f,z,t)$, expressed in cylindrical coordinates and as a function of time, was calculated from the system of equations:

$$(\lambda_n+2\mu_n)\nabla(\nabla\cdot U)-2\mu_n\nabla\cdot\nabla\cdot U + \rho_n A = \rho_n \frac{\partial^2 U}{\partial t^2} \quad (1)$$

where $(\nabla\cdot)$ is the first differential vector operator. λ_n and μ_n are elastic constants of layer n and ρ_n is the density of layer n.

The source, represented by the vector $A(r,z)$, acts at a point and is symmetric around a vertical axis. The components of A are

$$A_r = \frac{\partial}{\partial r}\left(\frac{\delta(r)}{r}\right) \sum_{k=1}^{K} q_k \, \delta(z-d_k) \sum_{l=1}^{L_k} f(t-\tau_{kl}) \quad (2)$$

$$A_z = \frac{\delta(r)}{r} \sum_{k=1}^{K} q_k \frac{d\delta(z-d_k)}{dz} \sum_{l=1}^{L_k} f(t-\tau_{kl}) \quad (3)$$

where the outer sum in each equation represents the number-time sequence of sources from one to K for different depths. q_k is the strength of a source and $\delta(z)$ is the delta function. The internal sum in each equation is summed over the number of sources from one to L_k. $f(t)$ is the explicit source time function, which is delayed in time by τ_{kl} for a source at depth d_k.

Some specific cases of equations (2) and (3) are

1. If $K=1$, $\tau_{11}=0$, $L_1=1$, then the source is a single impulse of form $f(t)$ at a depth $z=d_1$.

2. If $K=1$, $\tau_{11}\neq 0$, $L_1 = m$, then the source consist of a sequence of m impulses of form

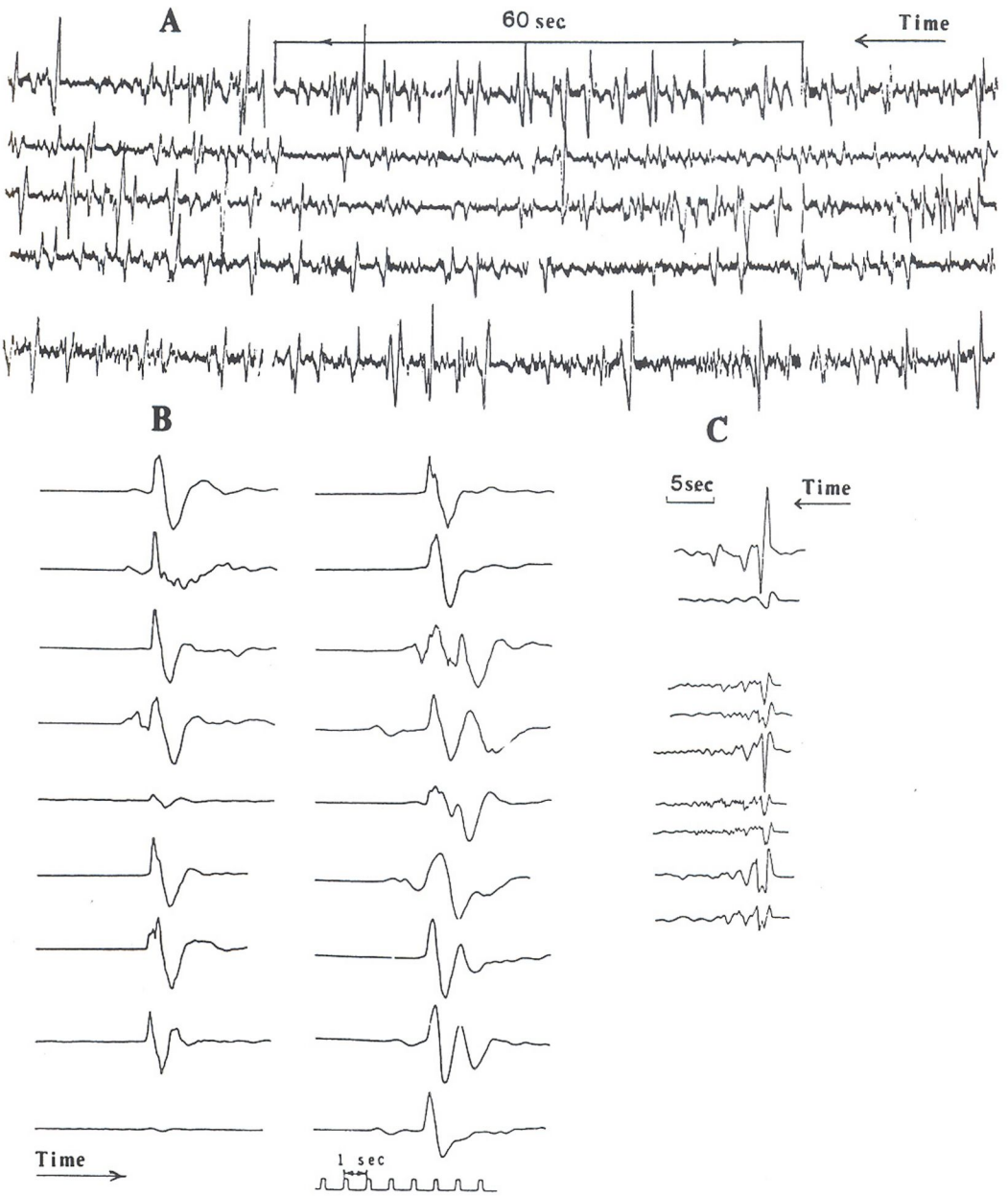

Fig. 1. Examples of acoustic recordings made during explosive eruptions. (a) north breakout of the Tolbachick fissure eruption, recording made in July 1975, 3.4 km from activity; (b) eruption of Tokachi-dake volcano, Hokkaido, Japan, recordings made between December 1988 and February 1989, about 3 km from activity [Okada et al., 1990]; and (c) eruption of Klyuchevskoy volcano, recording made between March and June 1983, 14.6 km from activity [Firstov and Storcheus, 1987].

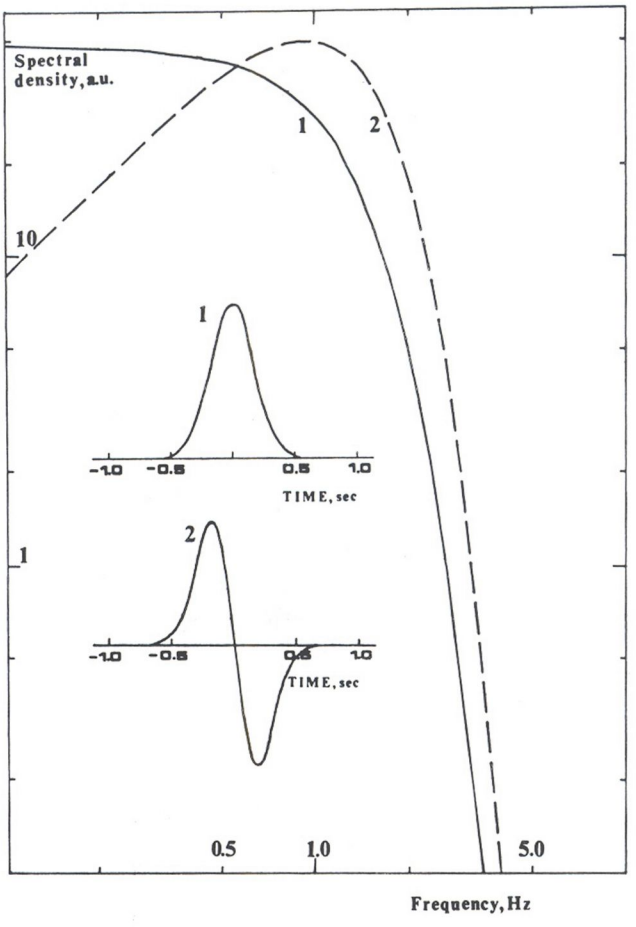

Fig. 2. Assumed shape of single impulse source: Curve 1, pressure change and curve 2, first derivative of pressure change.

f(t), succeeding ones occuring after a time delay of τ_{11}.

3. If all components of L=1, then the source consist of a set of K impulses distributed in space at depth $z=d_k$ and occuring after a time delay of τ_k .

In general, the source function is distributed arbitrarily in time and space, which includes having a source within any layer. The number of sources and time shifts is also arbitrary, although I have limited them to five. A similar construction of the source function was used by Chouet and Shaw [1991] and Shaw and Chouet [1991].

At this point, it is possible to form a complex source function out of the set of simple time functions f(t). The next step is to choose f(t).

Without a loss of generality, f(t) can be a single impulse because any complicated time function can be decomposed into a succession of single impulses. For a volcano, a single impulse would correspond to a single explosion. A sequence of explosions is considered as the sum of a sequence of single impulses delayed in time.

The exact form of f(t) is determined from records of atmospheric pressure waves produced by volcanic explosions [McNutt, 1986; Firstov and Storcheus, 1987; Okada et al., 1990]. Figure 1 shows pressure waves recorded during explosions at three different volcanoes. One feature in common with all three examples is the rapid rise of the initial portion of the pressure wave, possibly mimicking a rapid rise in pressure at the source. The remainder of the recorded pressure wave may be caused by dispertion of the acoustic wave in the atmosphere. One possible way to approximate a simple impulsive source is by an analytic expression of the form

$$f(t) = \exp\left(-\frac{(t-a)^2}{b^2}\right) \qquad (4)$$

where $a = \vartheta/2$ and $b = \vartheta/4.2$ and ϑ is a measure of the duration of the explosion. The well-known spectrum of f(t) is simply

$$S(\omega) = \frac{\sqrt{\pi}}{2}\, b \exp\left(-\left(\frac{b^2\omega^2}{4}\right)\right) \qquad (5)$$

Graphs of f(t) and S(ω) are shown in Figure 2, as well as the first derivative of both functions.

By using time delays, many different source functions can be constructed by combining individual impulses of the above form of f(t). I chose to model a harmonic source of frequency $1/\tau$ as a sequence of single impulses with a constant time shift of τ between each impulse. A similar model was used by Aki et al. [1977]. Figure 3 shows the specific source functions I used to calculate surface waveforms in a layered half-space. The first function was used earlier by Gordeev [1992] in a study of waveforms produced by a shallow tremor source. The third source function shown in Figure 3 consists of five single impulses shifted by 0.8 s, which corresponds to a frequency of 1.25 Hz.

Also shown in Figure 3 are theoretical seismograms calculated for a single low-velocity layer, of thickness 0.1 km, overlying half-space. The seismic velocities and densities used in my calculations are given in Table 1. The epicentral distance is given at the beginning of each seismogram in Figure 3. The source depth was 0.001 km. For each source function given in Figure 3, Figure 4 shows the spectra of the input function, the derivative of the input function, and the calculated theoretical seismogram.

Effects of Source Duration and Layer Thickness

Spectral bandwidth is inversely proportional to impulse duration. Figure 5 shows spectra produced by a single impulse of the form shown in Figure 3b, varying in duration from 0.25 s to 2 s. Again, the source depth was 0.001 km and the layer thickness was 0.1 km. The epicentral distance was 10 km. The spectra of the theoretical seismograms are narrower than the spectra of the source

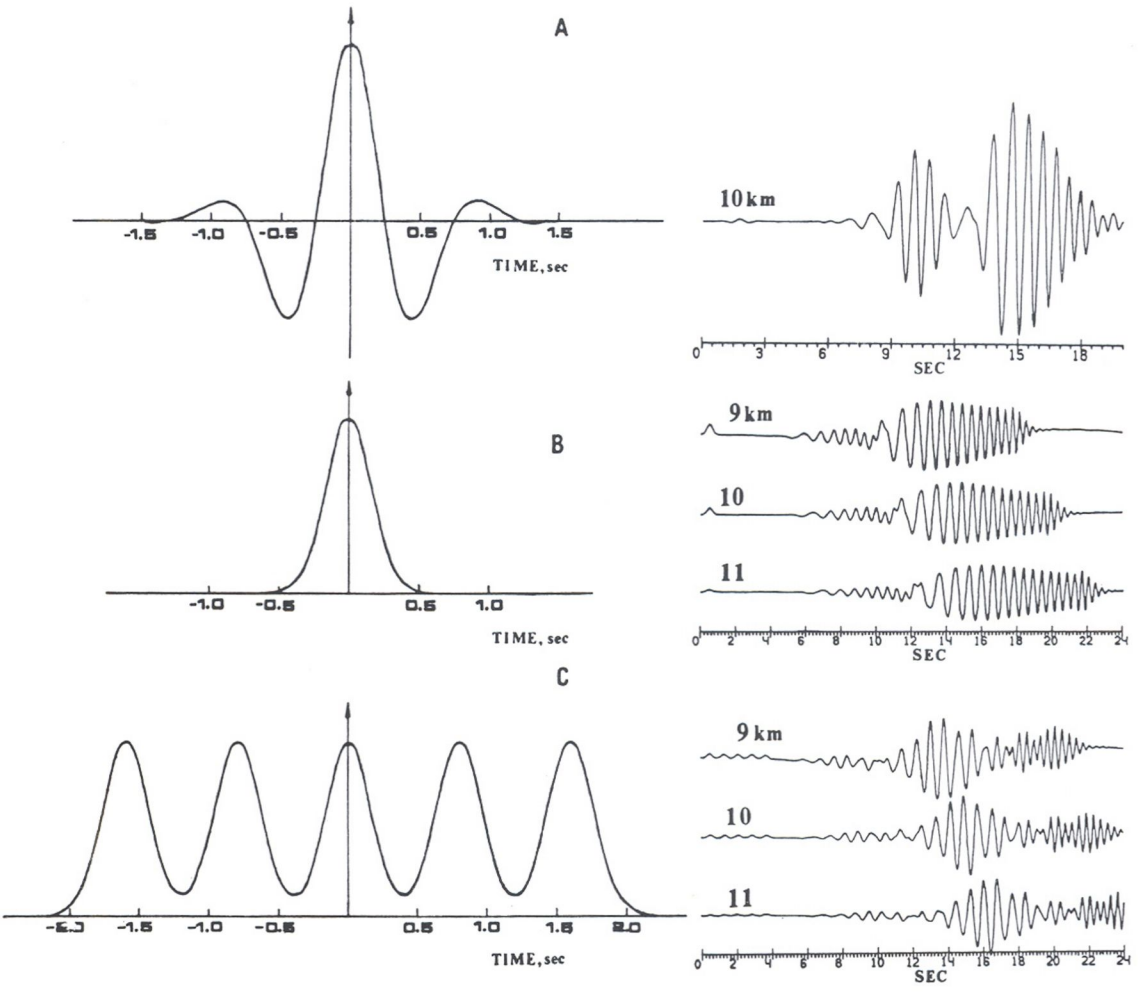

Fig. 3. (left) Three time source functions. (a) $f(t) = \exp[-2\pi f_0 (t-t_0)/\gamma^2] \cos[2\pi f_0 (t-t_0)]$ where f_0 is the frequency, $2t_0$ is the duration of the signal, γ is related to the decrease in amplitude with time. (b) $f(t) = \exp[-(t-a)^2/b^2]$, $a = \vartheta/2$, $b = \vartheta/4.2$ where ϑ is the duration of the signal. (c) $f(t) = \Sigma_{n=0}^{N} \exp[-(t-n\Delta t-a)^2/b^2]$, where a and b are the same as in (b). Δt is the time shift between successive impulses. (N+1) is the number of impulse sources. (right) Theoretical seismograms calculated for a single, low-velocity layer of thickness 0.1 km. Other model parameters are given in Table 1. Epicentral distances are given at the start of each seismogram.

function. The center frequency of a spectrum shifts to a lower value as the impulse duration increases.

Spectra of an actual acoustic recording of an explosion and the corresponding seismic recording are shown in Figure 6. These records were obtained at a distance of 3.5 km from an explosion of Tokachi-dake volcano, Hokkaido, Japan (provided by H. Okada of Usu Volcano Observatory). The acoustic and seismic recordings appear in the upper right corner. The spectra of the initial rise of the

TABLE 1. Parameters of the Low-Velocity Layer and Half-Space

	V_p, km/s	V_s, km/s	ρ, g/cm^3
Layer	1.0	0.7	1.4
Half-Space	2.0	1.15	1.6

V_p, velocity of the P waves; V_s, velocity of the S waves; ρ, densities.

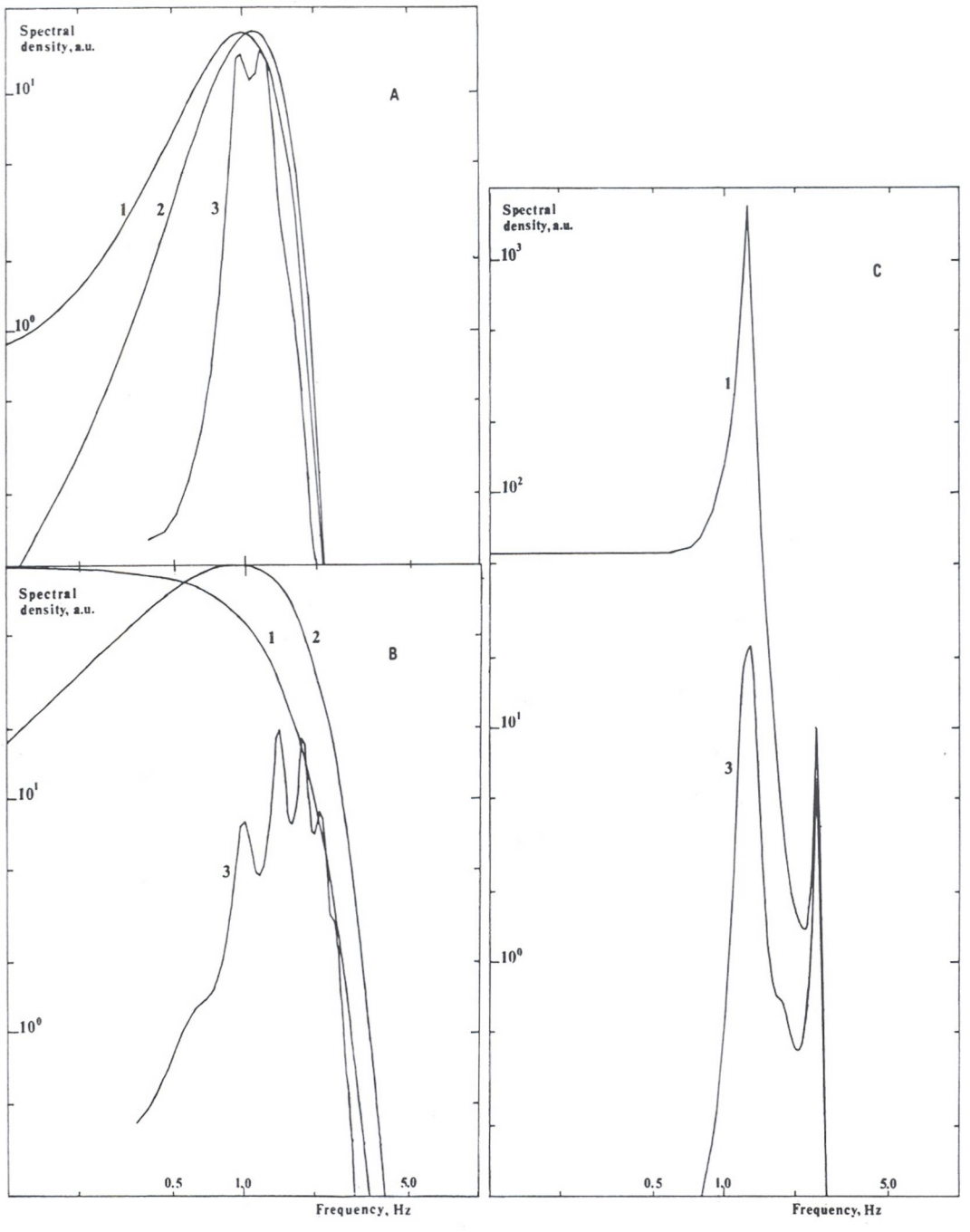

Fig. 4. The curves in each diagram are Curve 1, spectra of source functions; curve 2, the first derivative of source functions; and curve 3, spectra of theoretical seismograms calculated for an epicentral distance of 10 km. Figures 4a, 4b, and 4c correspond to the three source functions shown in Figure 3.

acoustic recording is identified in Figure 6 as curve 1; the spectra of the complete acoustic recording is identified as curve 2. The spectra of the seismic recording is identified as curve 3. Qualitatively, these spectra are similar to the theoretical spectra shown in Figure 5 for an impulse of 1-s duration.

It is possible to understand how the impedance contrast between the surface layer and the half-space affects waveforms produced by a single impulse by considering the theoretical seismograms calculated for surface layers of different thicknesses. Again, the seismic velocities and densities used in calculation are given in Table 1. In this illustration, the impulse duration is 1 s. From a comparison of the theoretical seismograms (all computed at an epicentral distance of 8 km for a shallow

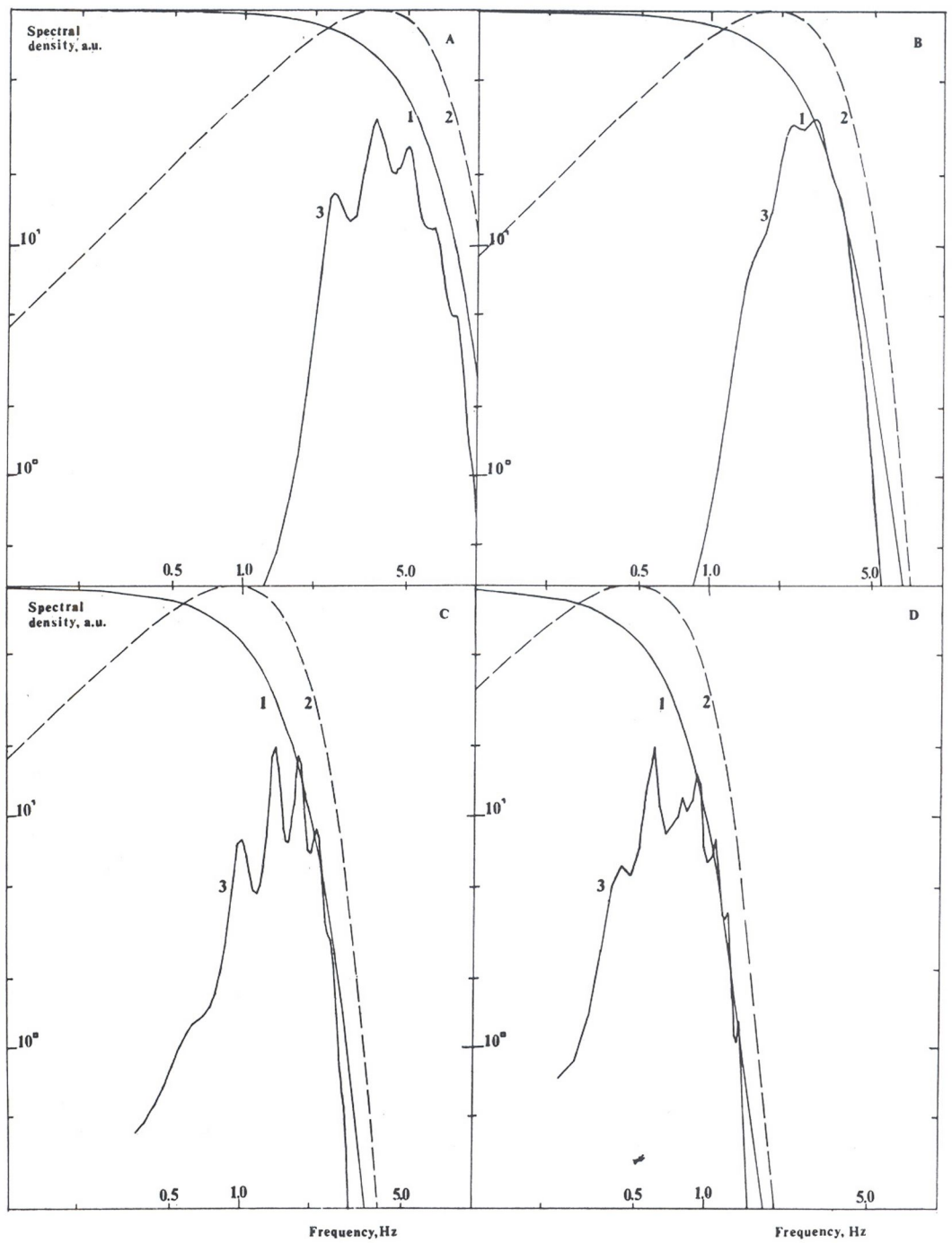

Fig. 5. As in Figure 4: Curve 1, spectra of source functions; curve 2, the first derivative of source functions; and curve 3, spectra of theoretical seismograms calculated for an epicentral distance of 10 km. The difference among these four boxes is the duration of the single impulse function (a) 0.25 s, (b) 0.5 s, (c) 1 s, and (d) 2 s.

source at a depth of 0.001 km) the effect of the surface layer is greatest when that layer is thin (Figure 7). In this specific example, the effect of the layer is insignificant if the layer is thicker than 1 km, and the shape of the theoretical seismogram takes the appearance of the half-space solution. The spectral peak of these seismograms shifts to high frequencies for the thinnest layers (Figure 8). The distribution of these peaks are identified in Figure 9 as a function of layer thickness. The amplitude of each

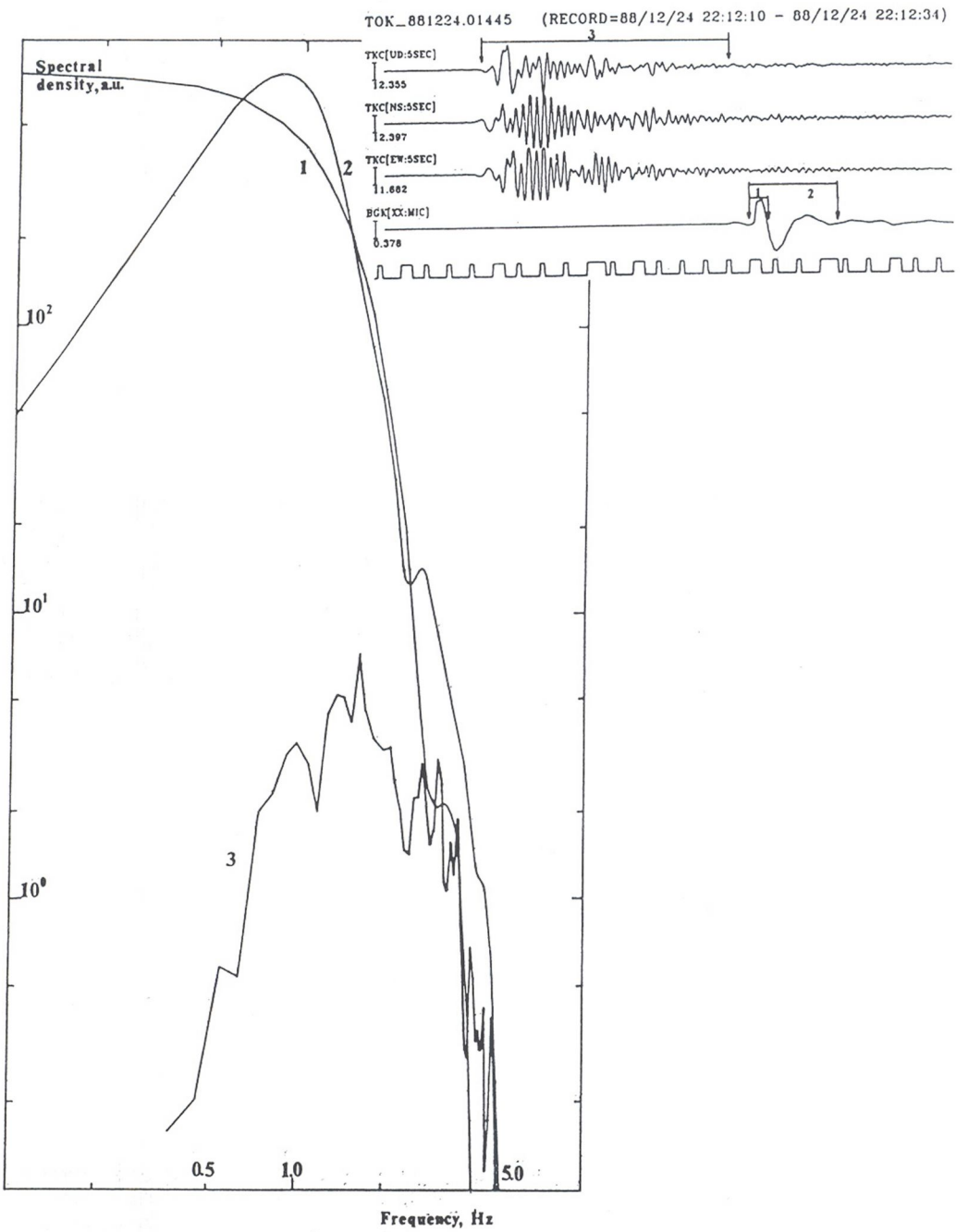

Fig. 6. Curve 1, spectra of the initial rise of the acoustic recording for the Tokachi-dake explosion (see Figure 1b); curve 2, spectra of the complete acoustic recording; and curve 3, spectra of vertical displacement recorded by a seismometer located about 2 km from the explosive crater. Acoustic and seismic recordings are shown in the upper right.

peak, relative to the largest peak for a specific layer thickness, is indicated by the size of the square.

Waveforms Produced by Harmonic Sources

The previous section shows how a sequence of single impulses can produce a harmonic source with a frequency determined by the time shift between impulses. For such harmonic sources, spectral peaks occur at integer intervals of the source frequency (Figure 4c).

Figure 10 shows the resultant source functions formed by sequences of single impulses with different time shifts. For impulses of 1-s duration, time shifts longer

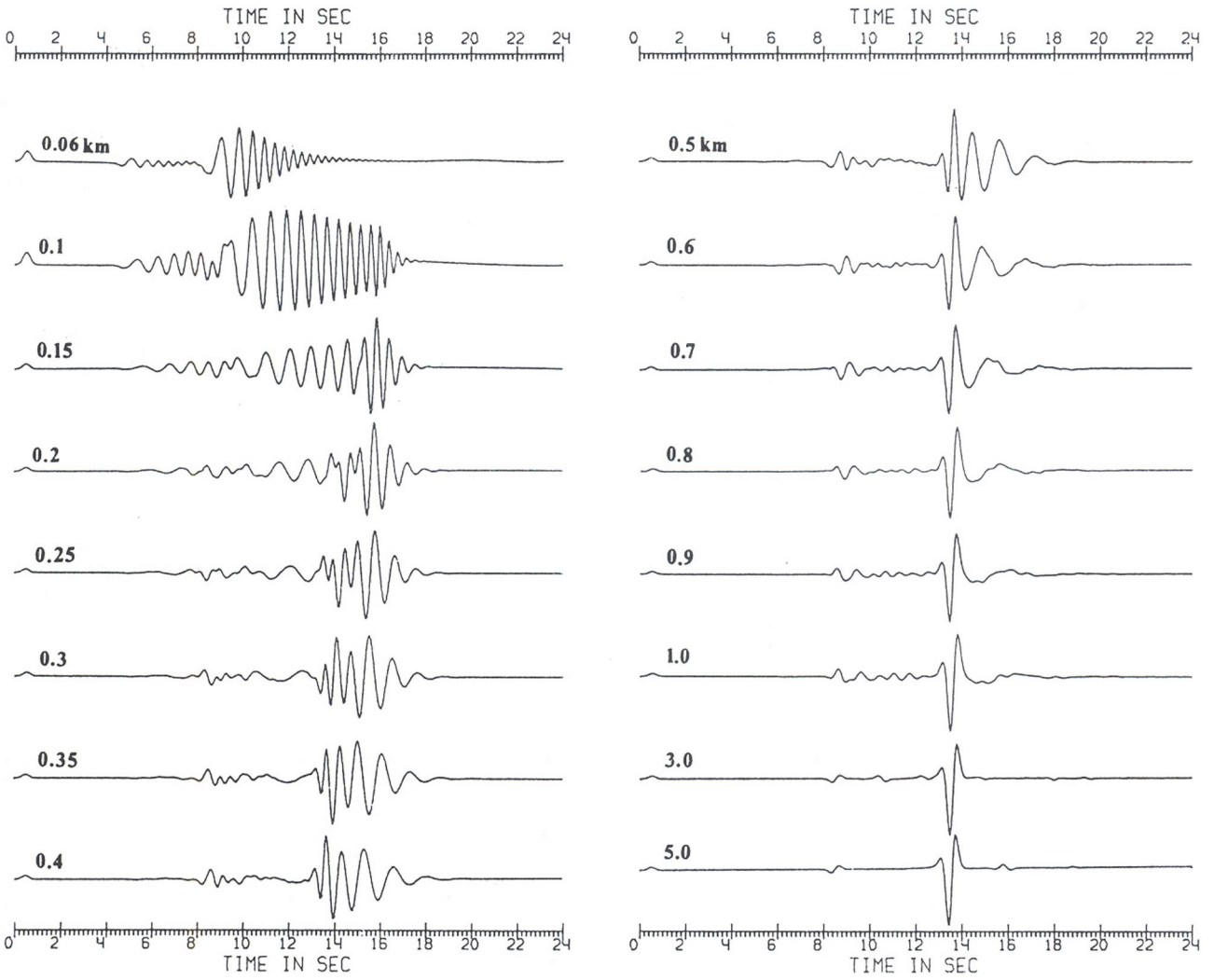

Fig. 7. Theoretical seismograms of radial displacement at an epicentral distance of 8 km. The seismic velocities and densities of the surface layer and half-space are given in Table 1. The source depth is 0.001 km. Each seismogram is parameterized by the thickness (in kilometers) of the surface layer.

than about 0.4 s produce a recognizable harmonic source. Time shifts longer than the signal duration, of course, produce a simple sequence of individual single impulses.

Theoretical seismograms for different time shifts are shown in Figure 11. These seismograms were calculated at an epicentral distance of 10 km. As in previous calculations, the layer thickness was 0.1 km and the source depth was 0.001 km. The seismic velocities and densities used in my calculations are given in Table 1. As the time shift increases, higher-frequency components appear in the seismograms. The first to appear is the second harmonic, which is delayed as a result of dispersal of Rayleigh waves. As the time shift continues to lengthen, so that it exceeds the source duration, which in this calculation was 1 s, the shape of the seismograms are controlled by interference of waves coming from individual impulses.

Theoretical seismograms calculated for harmonic sources are distinct in several important ways from seismograms calculated for a single impulse. When the time shift is short (in the example, less than about 0.2 s) so that the source is essentially a single wideband impulse, the seismogram consists of distinct wave packets. At slightly longer time shifts, 0.4 to 0.9 s, each wave packet has a characteristic frequency. This type of wave pattern, that consist of monochromatic oscillations of a long wave train, have been observed during some volcanic eruptions, which were, presumably, related to unstable two-phase flow. In these cases, the frequency of oscillation is related to the flow dynamics as well as the physical and chemical properties of the fluid.

Another wave pattern produced by shallow volcanic tremor is evident in the theoreti-

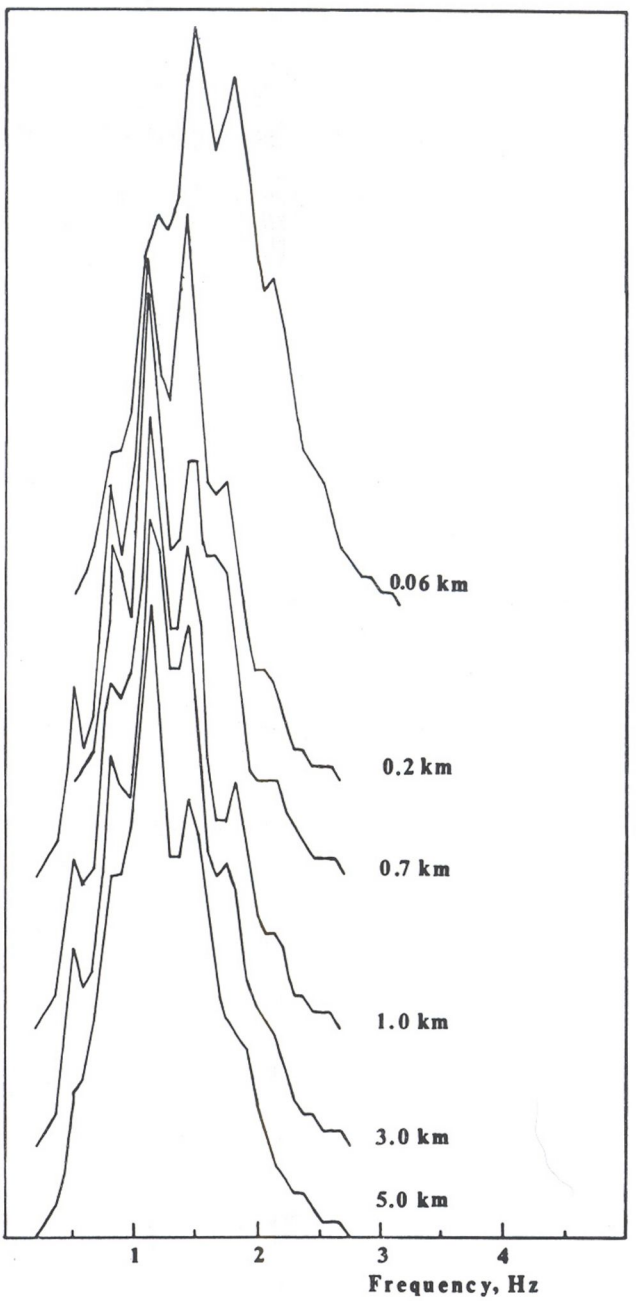

Fig. 8. Spectra of radial displacement of some theoretical seismograms shown in Figure 7. Each spectrum is parameterized by the thickness of the surface layer.

cal seismograms calculated for a sequence of individual impulses (in my example, time shifts longer than 2 s). As mentioned earlier, the seismograms are the result of interference of individual impulses, similar in appearance to sustained tremor during some volcanic eruptions, so that sustained tremor may be produced by a long sequence of individual explosions.

In summary, my model to calculate seismograms may explain many characteristics of seismic signals associated with volcanic explosions. The frequency range of the signals may be controlled by the spectra of an impulsive source. The possible existence of a surface layer has less effect on a sequence of individual impulses than on a wide-band source, which may be composed of many rapid impulses.

Effect of Material Parameters

So far, I have considered only models that have a single low-velocity layer with an impedance ratio of 2.29 between the layer and the lower half-space. The seismic velocities and densities of the layer and half-space are consistent with values expected for material that comprises volcanoes [Gordeev et al., 1990; Ferrazzini et al., 1991].

It is possible that in some cases the impedance contrast may be larger than 2.29. To illustrate the influence of larger contrast, in Figure 12 I calculated theoretical seismograms for different seismic velocities and densities of the surface layer and half-space, using a single impulse source of 1-s duration. Seismograms for a sequence of single 1-s impulses shifted by 0.5 s are shown in Figure 13. In all calculations, the thickness of the layer is still 0.1 km. Values of seismic velocities and densities are listed in Table 2.

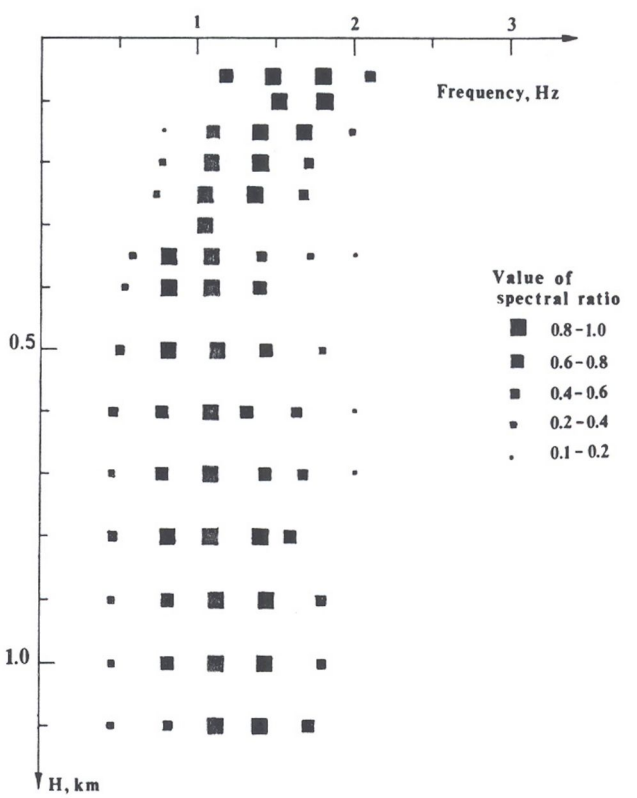

Fig. 9. Distribution of spectral peaks shown in Figure 8. Thickness of surface layer is shown on the vertical axis. The size of a square corresponds to the height af a spectral peak, normalized to the height of the maximum peak.

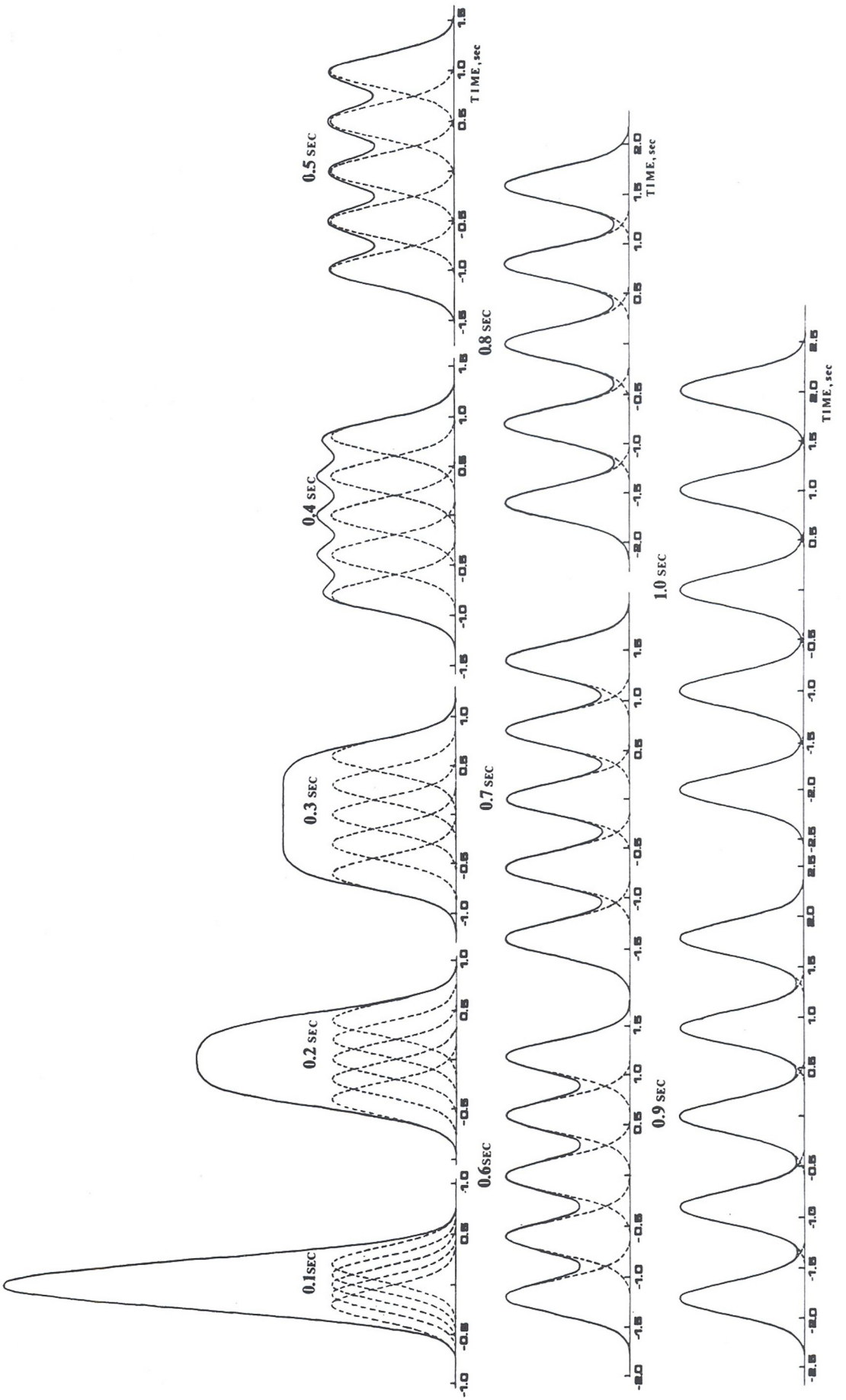

Fig. 10. Time source functions for various time shifts. A single impulse has a 1-s duration.

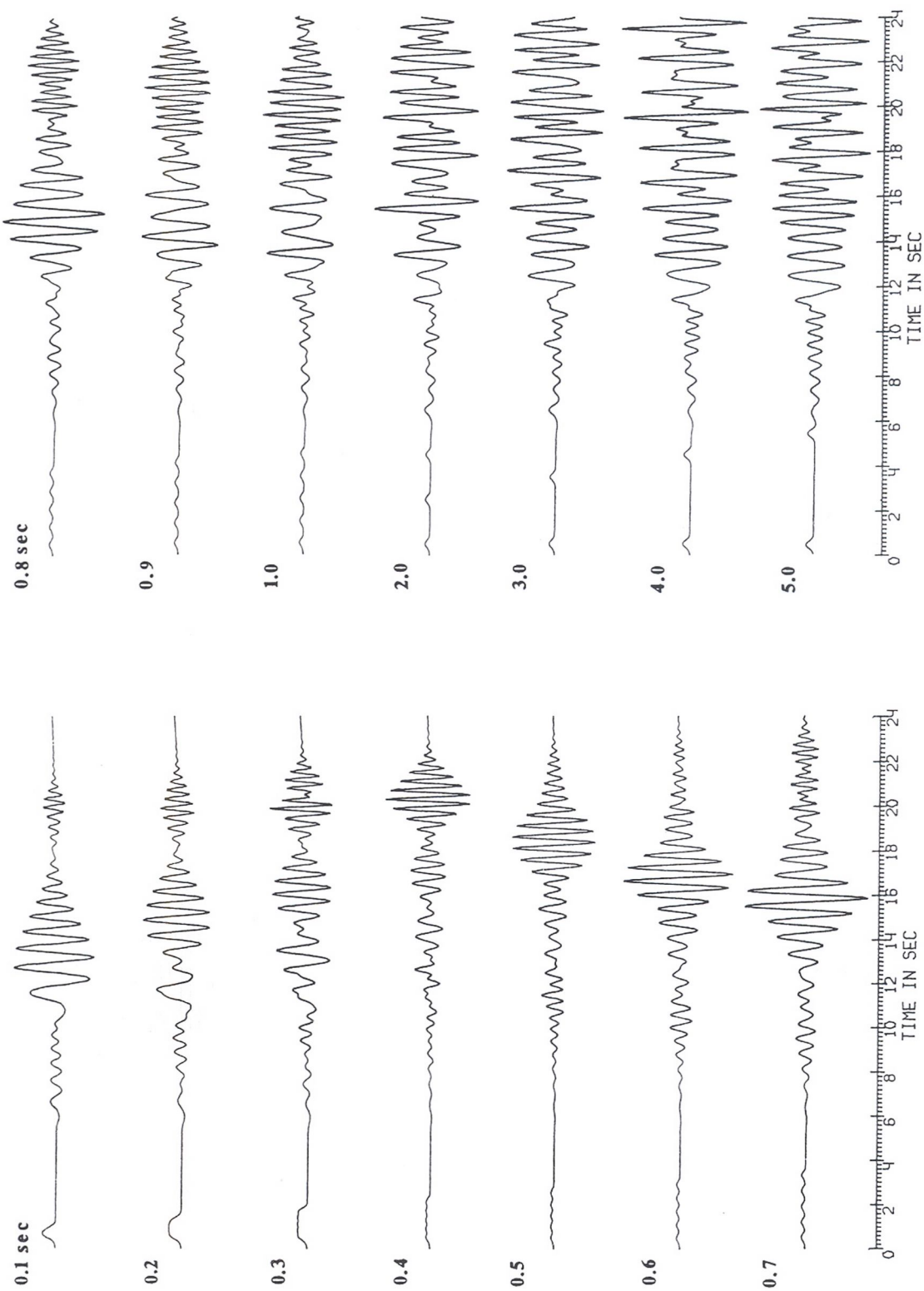

Fig. 11. Radial displacements of theoretical seismograms for a sequence of single impulses. Each seismogram is parameterized by the time shift between successive impulses. Epicentral distance is 10 km.

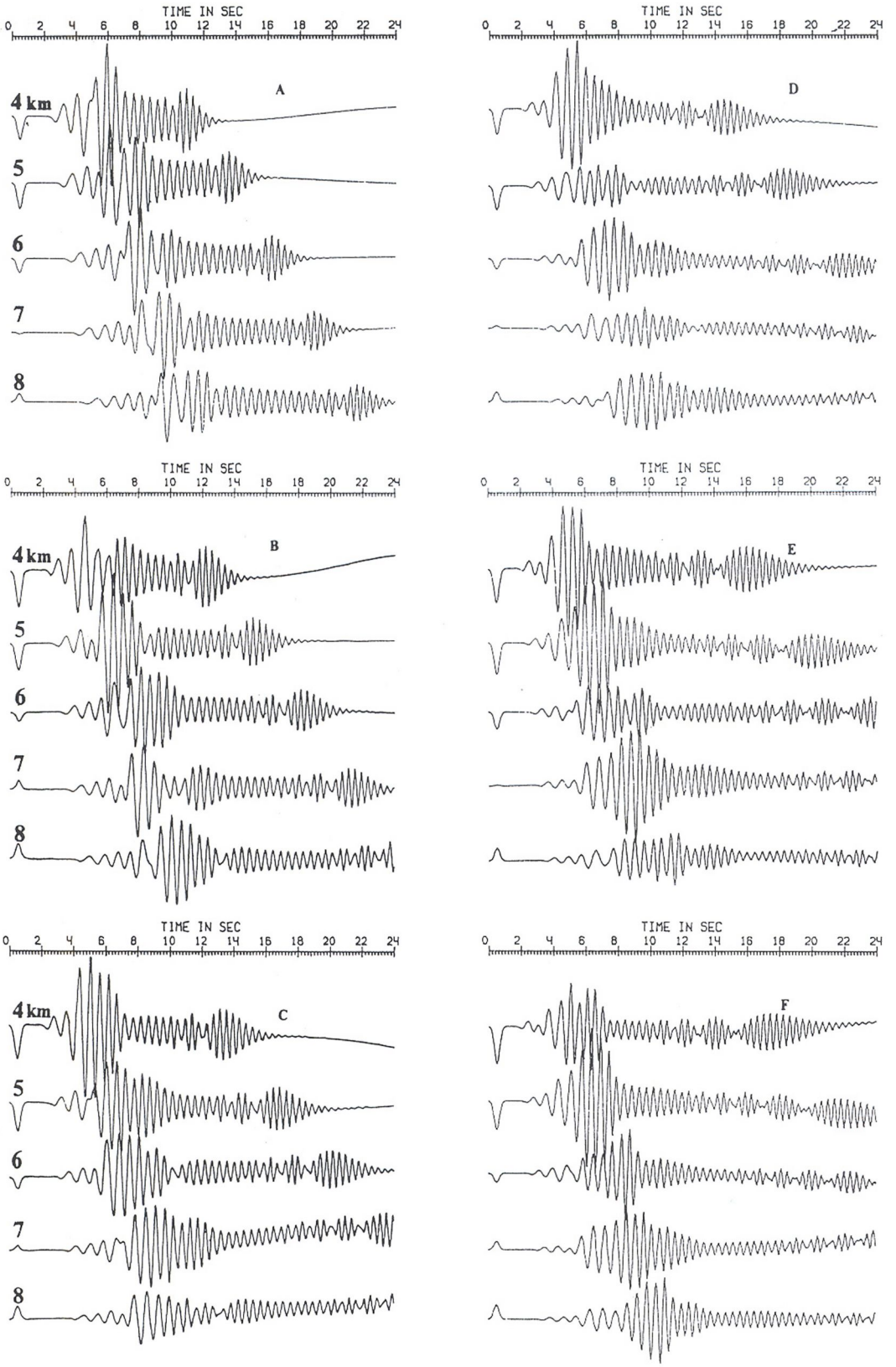

Fig 12. Theoretical seismograms of a single impulse for different values of seismic velocities and densities in the surface layer and half-space. These values are given in Table 2. Surface layer has a thickness of 0.1 km. Epicentral distance is given at the beginning of each seismogram.

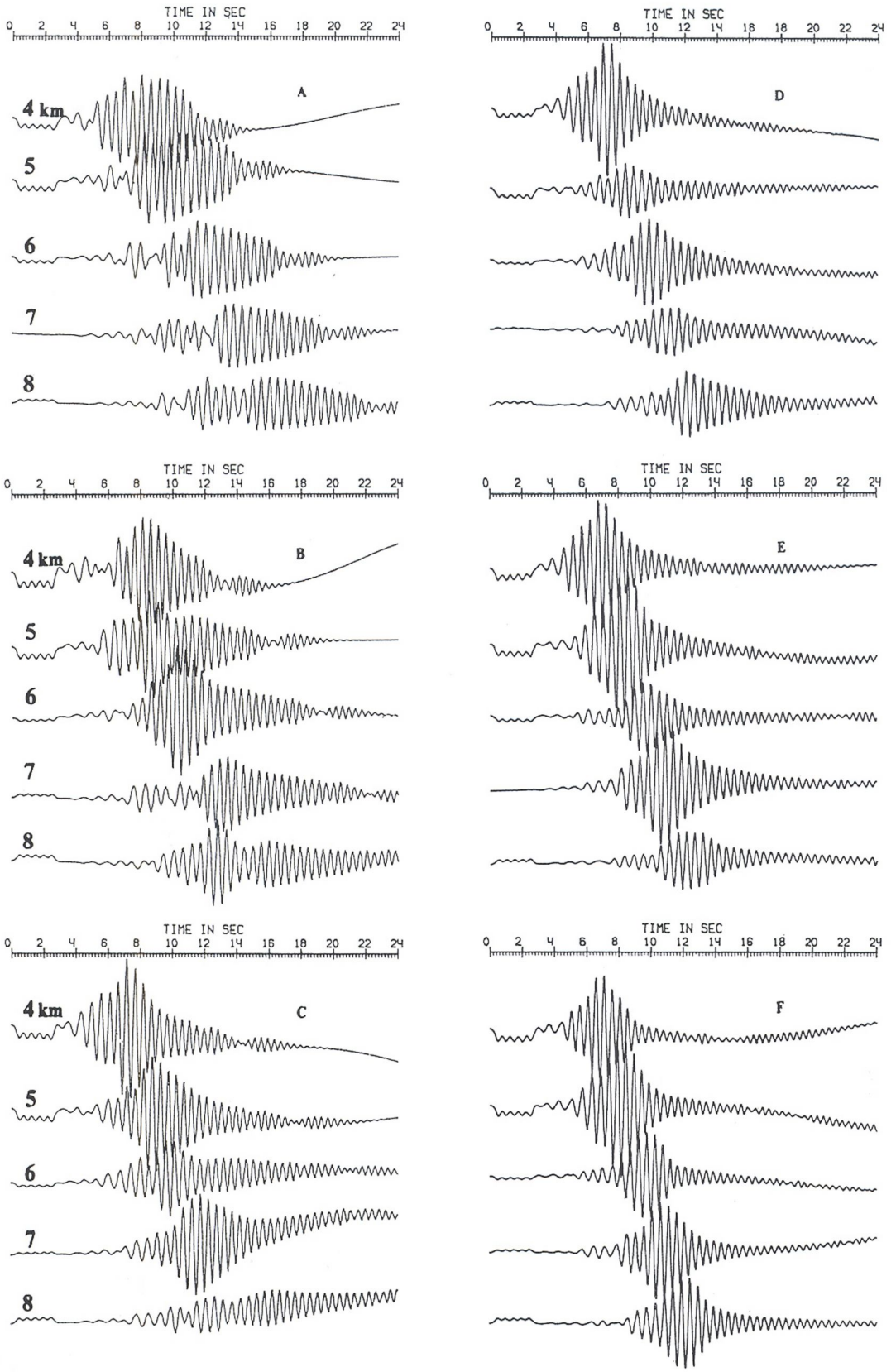

Fig. 13. Same as Figure 12, except for a sequence of five single impulses with a time shift of 0.5 s between successive pulses.

TABLE 2. Parameters of the Low-Velocity Layer and Half-Space

	Layer			Half-Space			Z_H/Z_L
	V_p, km/s	V_s, km/s	ρ, g/cm^3	V_p, km/s	V_s, km/s	ρ, g/cm^3	
A	1.0	0.58	1.4	2.0	1.16	1.6	2.29
B	1.0	0.58	1.4	2.2	1.27	2.0	3.14
C	1.0	0.58	1.4	2.4	1.39	2.2	3.77
D	1.0	0.58	1.4	2.6	1.50	2.4	4.46
E	1.0	0.58	1.4	2.8	1.62	2.6	5.20
F	1.0	0.58	1.4	3.0	1.73	2.8	6.00

V_p, velocity of the P waves; V_s, velocity of the S waves; ρ, densities; Z, impedances.

As the impedance increases between the layer and half-space, the duration of the seismogram increases, a result caused by more reflection at the bottom of the layer so that more energy remains in the layer.

In all the calculations I have presented, I used a very shallow source, at a depth of 0.001 km, only 1% of the layer thickness. This very shallow source means that most of the energy is transferred as surface waves. If the source depth is about a quarter wavelength of the P wave, almost equal energy is partitioned into body and surface waves; if the depth exceeds half the wavelength, most of the energy is transferred as body waves. This change in energy partitioning for deeper sources is illustrated in Figure 14, which shows the change in the relative amplitudes of surface waves (Rayleigh waves) and body waves (P waves). In this example, the low-velocity layer has a thickness of 1 km.

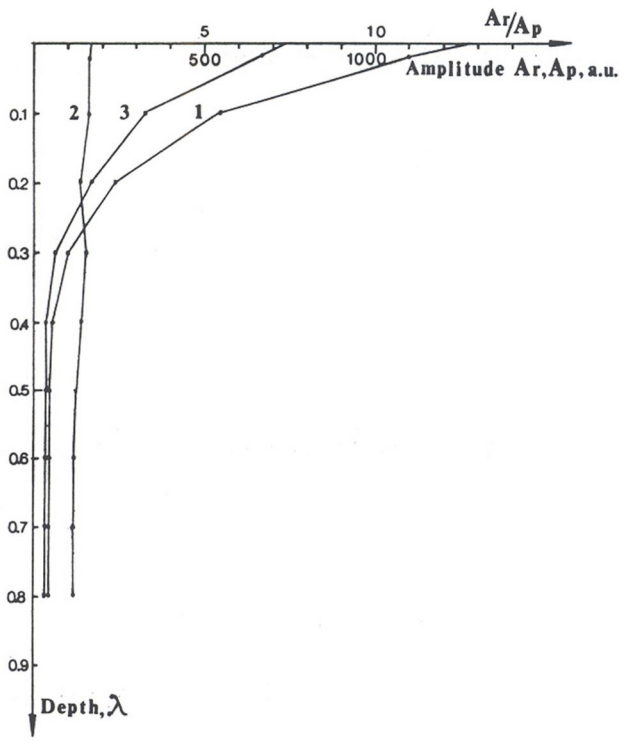

Fig. 14. Dependence of amplitudes of curve 1, surface waves (Rayleigh waves), and curve 2, body waves (P waves) as a function of depth of the source, in terms of seismic wavelength.

Theoretical seismograms for both radial and vertical component, as well as particle trajectories in a vertical plane, are shown in Figure 15 for various source depth, parameterized by the wavelength of the P wave. From these calculations, it is clear that surface waves dominate only for shallow sources, at depth less than 0.2 wavelengths. In Figure 16, the seismograms are for a surface layer of 0.1-km thickness. In this case, the amplitudes of body and surface waves are the same when the depth of the source is 0.5 wavelength; at larger depths, body waves dominate.

Conclusion

Several different sources may cause volcanic tremors. These include isolated gas explosions that occur during many eruptions. Where a thin low-velocity layer is present, such as a blanket of cinders or ash, a single explosive impulse will produce wave packets. The spectral content is controlled by the spectra of the source. If the source consist of a sequence of rapid, single impulses, which may occur as a result of several rapid explosions, the source function can be approximated as a single wide-band source. When the interval between impulses is comparable to the duration of a single impulse, the source function is nearly harmonic. In this case, the spectrum is completely determined by the harmonic character of the source. Such a situation may occur in two-phase flow, such as a gas and ash mixture or during degassing of magma [Chouet and Shaw, 1991].

Acknowledgments. I am very grateful to John Dvorak for great help in preparing this paper for publication. I thank also unknown referee for carefull corrections in English and helpful comments, which led to improvements of the manuscript.

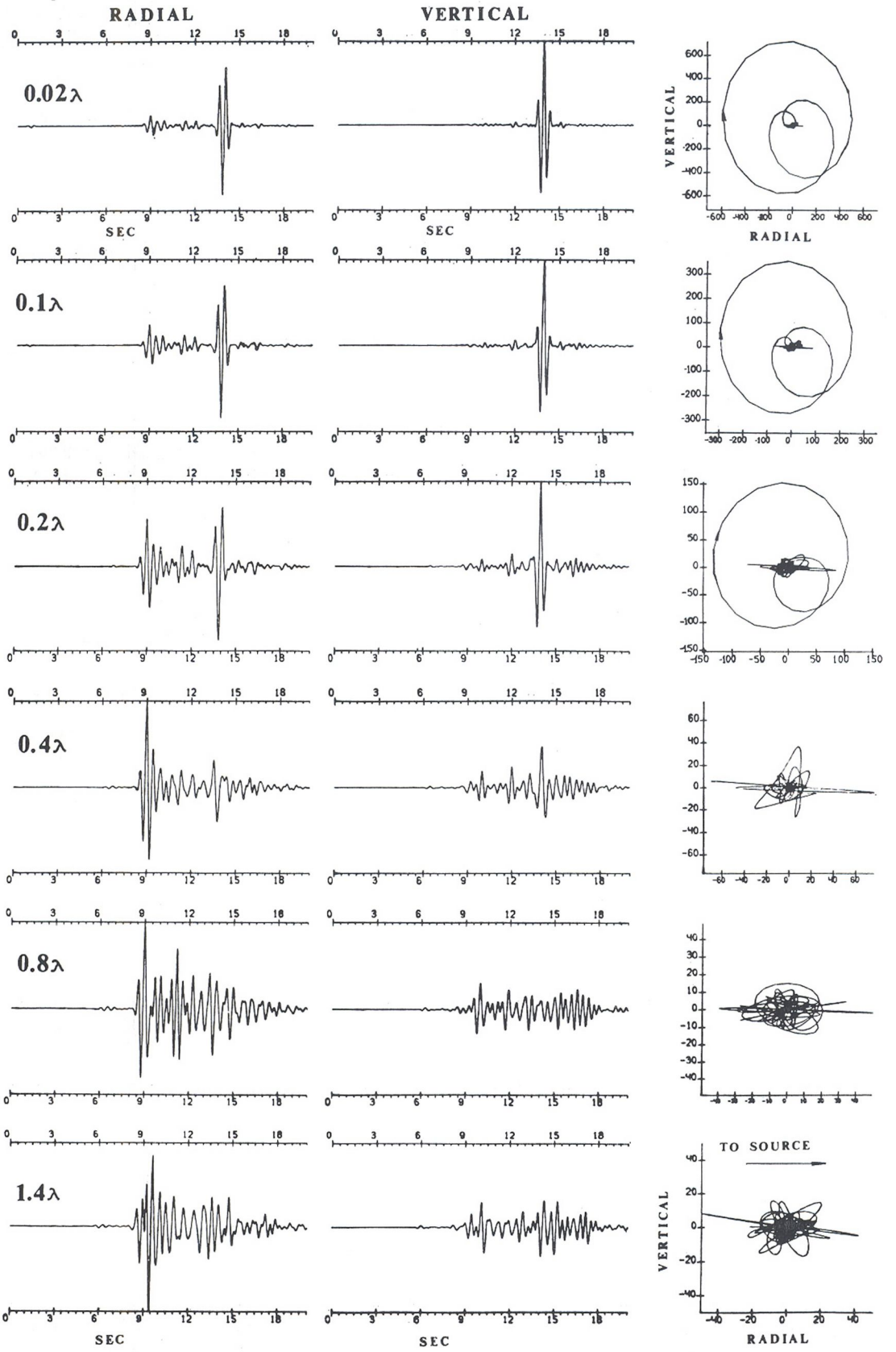

Fig. 15. Theoretical seismograms of radial and vertical displacements at an epicentral distance of 8 km. Particle trajectories in a vertical plane are shown at right. The depth of the source are given as units of wavelength of P waves in the surface layer.

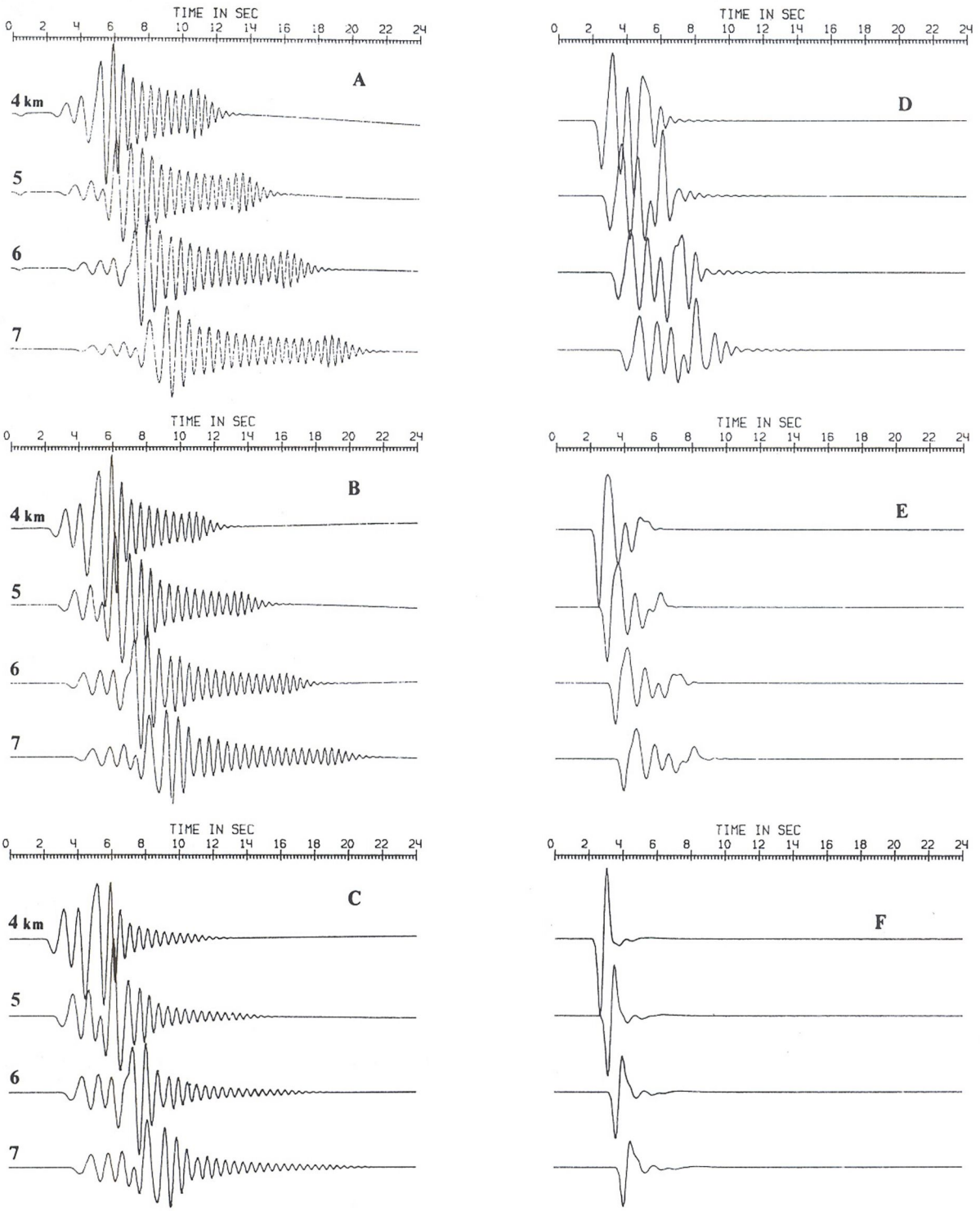

Fig. 16. Theoretical seismograms of radial displacements for various thicknesses of the surface layer, expressed in terms of the wavelength, l, of the P wave. (a) 0.05 λ, (b) 0.1 λ, (c) 0.2 λ, (d) 0.5 λ, (e) 1.0 λ, (f) 2.0 λ. Depth of the source is given at the beginning of each seismogram.

References

Aki, K., and R. Y. Koyanagi, Deep volcanic tremor and magma ascent mechanism under Kilauea, Hawaii, *J. Geophys. Res.*, *86*, 7095-7110, 1981.

Aki, K., M. Fehler, and S. Das, Source mechanism of volcanic tremor: fluid-driven crack models and their appli-cation to the 1963 Kilauea eruption, *J. Volcanol. Geotherm. Res.*, *2*, 259-287, 1977.

Chouet, B., Ground motion in the near field of a fluid-driven crack and its interpretation in the study of shallow volcanic tremor, *J. Geophys. Res.*, *86*, 5985-6016, 1981.

Chouet, B., Excitation of a buried magmatic pipe: A seismic source model for volcanic tremor, *J. Geophys. Res.*, *90*, 1881-1893, 1985.

Chouet, B., Resonance of a fluid-driven crack: radiation properties and implications for the source of long-period events and harmonic tremor, *J. Geophys. Res.*, *93*, 4373-4400, 1988.

Chouet, B., and H. R Shaw, Fractal properties of tremor and gas-piston events observed at Kilauea Volcano, Hawaii, *J. Geophys. Res.*, *96*, 10,177-10,189, 1991.

Cosentino, M., G. Lombardo, G. Patane, R. Schick, and A. D. L. Sharp, Seismological research on Mt.Etna: State of art and recent trends, *Mem. Soc. Geol. Ital.*, *23*, 159-202, 1982.

Crosson, R.S., and D.A. Bame, A spherical source model for low-frequency volcanic earthquakes, *J. Geophys. Res.*, *90*, 10,237-10,247, 1985.

Fatyanov, A.G., Lamb numeric solution for unelastic inhomogeneous of Boltsman, in *Numeric Methods for Interpretation of Geophysical Observations* (in Russian), pp 144-156, edited by A. Alekseev, Novosibirsk, Russia, 1980.

Fatyanov, A.G., and B.G. Mikhailenko, A method for calculation of non-stationary wave fields in laminated heterogeneous media (in Russian), *Doklady Academii Nauk USSR*, *301*, 834-839, 1988.

Ferrazzini, V., K. Aki, and B. Chouet, Characteristics of seismic waves composing Hawaiian volcanic tremor and gas-piston events observed by a near-source array, *J. Geophys. Res.*, *96*, 6199-6209, 1991.

Ferrick, M. G., A. Qamar, and W. F. St.Lawrence, Source mechanism of volcanic tremor, *J. Geophys. Res.*, *87*, 8675-8683, 1982.

Firstov, P. P., and A. V. Storcheus, Acoustic signals that accompanied the March-June 1983 eruption at Klyuchevskoy volcano (in Russian), *Volcanol. Seismol.*, *5*, 66-80, 1987.

Gordeev, E. I., V. A. Saltykov, V. I. Sinitsyn, and V. N. Chebrov, Temporal and spatial characteristics of volcanic tremor wave fields, *J. Volcanol. Geotherm. Res.*, *40*, 89-101, 1990.

Gordeev, E. I., Modeling of volcanic tremor wave fields, *J. Volcanol. Geotherm. Res.*, *51*, 145-160, 1992.

Jaeger, J. C., *Elasticity, Fracture and Flow with Engineering and Geological Applications*, 268 pp., John Wiley, New York, 1969.

Kubotera, A., Volcanic tremor at Usu volcano, in *Physical Volcanology, Developments in Solid Earth Geophysics*, edited by L. Civetta et al., pp 29-47, Elsevier, New York, 1974.

McNutt, S. R., Observations and analysis of b-type earthquakes, explosions and volcanic tremor at Pavloff volcano, Alaska, *Bull. Seismol. Soc. Am.*, *76*, 153-175, 1986.

Minakami, T., Earthquakes and crustal deformations originating from volcanic activities, *Bull. Earthquake Res. Inst. Univ. Tokyo*, *38*, 497-544, 1960.

Okada, H., Y. Nishimura, H. Miyamachi, H. Mori, and K. Ishihara, Geophysical significance of the 1988-1989 explosive of Mt. Tokachi, Hokkaido, Japan, *Bull. Volcanol. Soc. Jpn.*, *35*, 175-203, 1990.

Schick, R., Volcanic tremor-source mechanisms and correlation with eruptive activity, *Nat. Hazard*, *1*, 125-144, 1988.

Seidl, D., R. Schick, and M. Riuscetti, Volcanic tremors at Etna: A model for hydraulic origin, *Bull. Volcanol.*, *44*, 43-55, 1981.

Shaw, H. R., and B. Chouet, Fractal hierarchies of magma transport in Hawaii and critical self-organization of tremor, *J. Geophys. Res.*, *96*, 10,191-10,207, 1991.

St.Lawrence, W. F., and A. Qamar, Hydraulic transients: A seismic source in volcanoes and glaciers, *Science*, *203*, 654-656, 1979.

E. I. Gordeev, Institute of Volcanology, Far East Division, Russian Academy of Science, A. Pijp, 9, 683006, Petropavlovsk-Kamchatsky, Russia.

(Received April 27, 1992;
revised February 2, 1993;
accepted February 5, 1993.)